catalysts

MDPI

Article

Enhancing Soluble Expression of Phospholipase B for Efficient Catalytic Synthesis of L-Alpha-Glycerylphosphorylcholine

Jiao Feng, Wenjing Yang, Yuanyuan Lu, Hui Li, Sheng Xu, Xin Wang * and Kequan Chen

State Key Laboratory of Materials-Oriented Chemical Engineering, College of Biotechnology and Pharmaceutical Engineering, Nanjing Tech University, Nanjing 211816, China; fengjiao88@njtech.edu.cn (J.F.); yangwenjing1128@126.com (W.Y.); lyy940812@163.com (Y.L.); lihui11@njtech.edu.cn (H.L.); henryxu@njtech.edu.cn (S.X.); kqchen@njtech.edu.cn (K.C.)
* Correspondence: xinwang1988@njtech.edu.cn

Abstract: Phospholipase B (PLB) harbors three distinct activities with broad substrate specificities and application fields. Its hydrolyzing of sn-1 and sn-2 acyl ester bonds enables it to catalyze the production of L-alpha-glycerylphosphorylcholine (L-α-GPC) from phosphatidylcholine (PC) without speed-limiting acyl migration. This work was intended to obtain high-level active PLB and apply it to establish an efficient system for L-α-GPC synthesis. PLB from *Pseudomonas fluorescens* was co-expressed with five different molecular chaperones, including trigger factor (Tf), GroEL-GroES (GroELS), DnaK-DnaJ-GrpE (DnaKJE), GroELS and DnaKJE, or GroELS and Tf or fused with maltose binding protein (MBP) in *Escherichia coli* BL21(DE3) to improve PLB expression. PLB with DnaKJE-assisted expression exhibited the highest catalytic activity. Further optimization of the expression conditions identified an optimal induction OD_{600} of 0.8, IPTG concentration of 0.3 mmol/L, induction time of 9 h, and temperature of 25 °C. The PLB activity reached a maximum of 524.64 ± 3.28 U/mg under optimal conditions. Subsequently, to establish an efficient PLB-catalyzed system for L-α-GPC synthesis, a series of organic-aqueous mixed systems and surfactant-supplemented aqueous systems were designed and constructed. Furthermore, the factors of temperature, reaction pH, metal ions, and substrate concentration were further systematically identified. Finally, a high yield of 90.50 ± 2.21% was obtained in a Span 60-supplemented aqueous system at 40 °C and pH 6.0 with 0.1 mmol/L of Mg^{2+}. The proposed cost-effective PLB production and an environmentally friendly PLB-catalyzed system offer a candidate strategy for the industrial production of L-α-GPC.

Keywords: phospholipase B; soluble expression; *Escherichia coli*; biocatalysis; L-alpha-glycerylphosphorylcholine

Citation: Feng, J.; Yang, W.; Lu, Y.; Li, H.; Xu, S.; Wang, X.; Chen, K. Enhancing Soluble Expression of Phospholipase B for Efficient Catalytic Synthesis of L-Alpha-Glycerylphosphorylcholine. *Catalysts* **2022**, *12*, 650. https://doi.org/10.3390/catal12060650

Academic Editors: Anwar Sunna and Richard Daniellou

Received: 22 April 2022
Accepted: 10 June 2022
Published: 13 June 2022

1. Introduction

L-alpha-glycerylphosphorylcholine (L-α-GPC) is a choline compound and an essential precursor of phosphatidylcholine (PC), acetylcholine, and membrane phospholipid [1,2]. Its ability to alleviate cognitive impairment and promote memory has been applied to effectively treat Alzheimer's disease, dementia, and other neurodegenerative diseases [3,4]. Hence, L-α-GPC has promising application prospects in medicine, pharmaceuticals, food, and cosmetics [4,5]. It has been reported that L-α-GPC can be produced by extraction, as well as chemical and enzymatic methods [2]. In contrast to the low yield of extraction and the toxicity and environmental pollution associated with chemical methods, production of L-α-GPC by enzyme catalysis is a promising method for industrial application with significant advantages, including environmental friendliness, high efficiency, specific catalytic process, and a more comprehensive range of flexible reaction conditions [6,7].

L-α-GPC has been reported to be synthesized successfully by several enzymatic methods. *Rhizomucor miehei* lipase (RML) was reported to catalyze transesterification of L-dipalmitoylphosphatidylcholine by employing cis-5,8,11,14,17-eicosapentaenoic acid to afford L-α-GPC [8]. The most important and widely used method is the hydrolysis of PC

to synthesize L-α-GPC by phospholipases, including phospholipase A_1 (PLA_1, EC 3.1.1.32) and a few phospholipase Bs (PLBs, EC 3.1.1.5) [2,6,9,10]. PLA_1 is the most commonly used enzyme harboring the hydrolytic activity to phospholipids at the sn-1 position. In the PLA_1-catalyzed reaction to synthesize L-α-GPC, the acyl group from the sn-1 position of PC is first hydrolyzed by PLA_1; then, the acyl group from the sn-2 position is converted into the sn-1 position through acyl migration, and finally, L-α-GPC is synthesized by further hydrolysis (Scheme 1) [7]. The slow acyl migration rate is one of the significant constraints on the industrial production of L-α-GPC by PLA_1 [10,11]. PLB can act as a fatty acid ester hydrolase, a lysophospholipase, or a transacylase [12]. Its activity as the hydrolase cleaving at both sn-1 and sn-2 acyl ester bonds can dispense with the slow acyl migration from the sn-2 position to the sn-1 position. The variety of different activities of PLB make it suitable for a wide range of applications and increasingly important in industrial processes, such as the production of phospholipid derivatives and degumming of vegetable oils [6,13,14]. PLBs derived from bacteria, fungi, plants, and mammalian cells have been wildly identified, and some of them have been successfully cloned in heterologous expression systems [15–17]. For commercial applications, producing PLB in large quantities is difficult due to its low expression level and ease of existing in the form of inclusion bodies [12]. Therefore, a high-level PLB production system or technology is required.

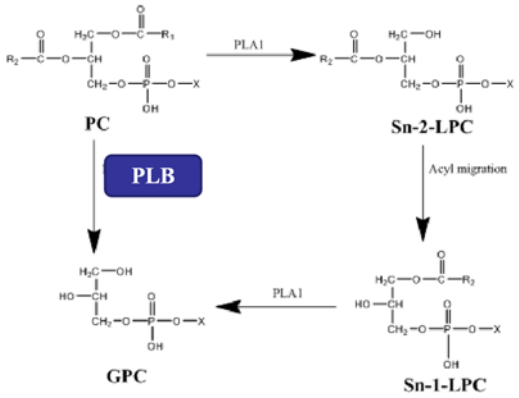

Scheme 1. Schematic of L-α-GPC enzymatic production from PC [2,7].

In recent years, a few PLBs have been attempted to synthesize L-α-GPC directly in boric acid-NaOH buffer or Tris-HCl buffer [2,6]. However, the low solubility of substrate PC in the aqueous phase caused by its lipophilic feature is a crucial obstacle to the high productivity of L-α-GPC and large-scale preparation [11,18]. For PLA_1-catalyzed hydrolysis, an organic-aqueous biphasic system (*n*-hexane-water biphasic medium), water-in-oil system, and Tween 20 aqueous reaction system were developed to improve the solubility of PC and achieve good catalytic efficiencies with high L-α-GPC productivity [7,18,19]. In contrast to the well-studied reaction systems of PLA_1, few studies have focused on the properties of PBL to construct an effective PLB-catalyzed hydrolysis system to synthesize L-α-GPC.

Based on the above, the objective of this work was to develop an expression strategy for high-level production of active PLB and a reaction system to achieve efficient PLB-catalyzed synthesis of L-α-GPC. PLB from *Pseudomonas fluorescens* was heterologously expressed in *Escherichia coli* BL21(DE3). Moreover, fusion partner maltose-binding protein (MBP) and different molecular chaperones, including trigger factor (Tf), GroEL-GroES (GroELS), DnaK-DnaJ-GrpE (DnaKJE), GroELS and DnaKJE, or GroELS and Tf, were fused or co-expressed with PLB to facilitate the soluble expression of PLB in *E. coli* BL21(DE3). Following optimization of expression conditions, the purified PLB was used to produce L-α-GPC. Subsequently, a series of organic-aqueous mixed systems and surfactant-supplemented aqueous systems were designed and constructed to explore the PLB-catalyzed synthesis of L-α-GPC. Finally, the factors of temperature, reaction pH, metal ions, and substrate concentration were further systematically identified.

2. Results and Discussion

2.1. Expression of Recombinant PLB in E. coli BL21(DE3)

Several different sources of PLB have been identified, among which PLB from *P. fluorescens* exhibited higher catalytic activity [12]. In this work, the codon-optimized coding sequence of PLB from *P. fluorescens* was ligated to pET 28a to construct the recombinant expression vector pET28a-PLB. Then, *E. coli* was used as the recombinant protein expression system for heterologous PLB production. The pET 28a-PLB was transformed into *E. coli* BL21(DE3) to the recombinant *E. coli* BL21(DE3)/pET 28a-PLB. After cell disruption, the soluble supernatant and insoluble cell debris were analyzed by SDS–PAGE analysis (Figure 1). It was found that a band of about 46 kDa corresponded to the molecular weight of PLB [12]. However, the visible target band of insoluble cell debris indicated that inclusion bodies were formed during the expression of recombinant PLB. Overexpression of protein at a low induction level and a low temperature can usually improve the solubility and activity of recombinant protein [20]. However, even at the low induction temperature of 20 °C and the low IPTG concentration of 0.1 mM, the insoluble cell debris was also found to contain inclusion bodies in our work. The results suggest that the recombinant PLB was primarily expressed as insoluble inclusion bodies. The inclusion body formation resulted in lower enzyme activity of the PLB. The activity of the crude enzyme was only 17.50 ± 3.53 U/mg. Saturated protein folding machinery promotes protein misfolding and aggregation during overexpression of the recombinant protein, known as inclusion bodies [21].

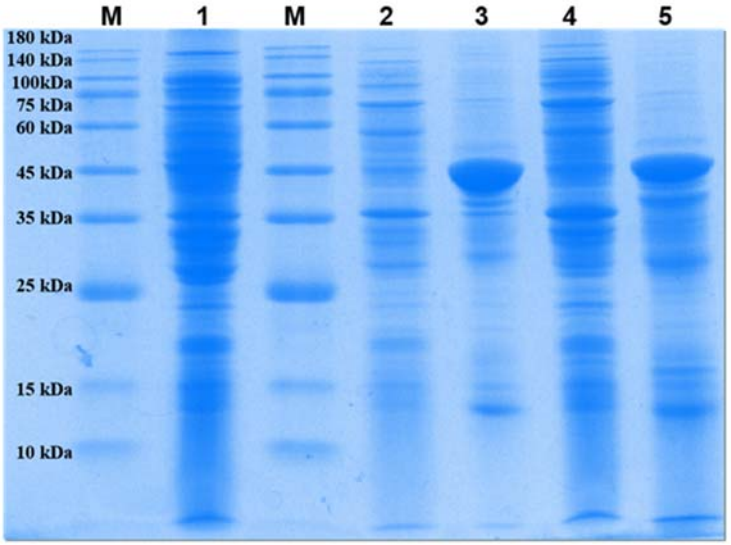

Figure 1. SDS-PAGE analysis of PLB expressed in *E. coli* BL21(DE3). Lane M: protein molecular weight marker; lane 1: supernatant of *E. coli* BL21(DE3); lane 2: supernatant of *E. coli* BL21(DE3)/pET28a-PLB induced at 30 °C with 0.5 mM of IPTG; lane 3: precipitation of *E. coli* BL21(DE3)/pET28a-PLB induced at 30 °C with 0.5 mM of IPTG; lane 4: supernatant of *E. coli* BL21(DE3)/pET28a-PLB induced at 20 °C with 0.1 mM of IPTG; lane 5: precipitation of *E. coli* BL21(DE3)/pET28a-PLB induced at 20 °C with 0.1 mM of IPTG.

2.2. Promoting the Soluble Expression of PLB with the Assistance of Molecular Chaperones

The formation of inclusion bodies limited the high-throughput production and enzyme activity of recombinant PLB. To minimize inclusion body formation, the highly soluble maltose-binding protein (MBP, about 40 kDa) was used as tagged proteins fused to the N terminus of PLB. As shown in Figure 2a, the protein band of MBP-fused PLB was detected at a molecular weight of about 87 kDa on the SDS–PAGE gel, and MBP tag slightly enhanced the solubility of PLB. It has been proposed that MBP serves as a "molecular chaperone" to prevent self-aggregation [22] or acts as a "holdase" to assist in proper folding [23,24]. To investigate the influence of MBP tags on the enzyme activity of PLB, MBP-fused PLB was

purified by amylose affinity chromatography; then, purified PLB was obtained by cleaving from MBP with the specific protease Factor Xa. Enzyme activities of MBP-fused PLB and PLB cleaved from MBP were 51.41 ± 2.94 U/mg and 86.98 ± 0.92 U/mg, respectively (Figure 2b). The results indicate that MBP, as a fusion partner, promoted soluble expression and enzyme activity of PLB.

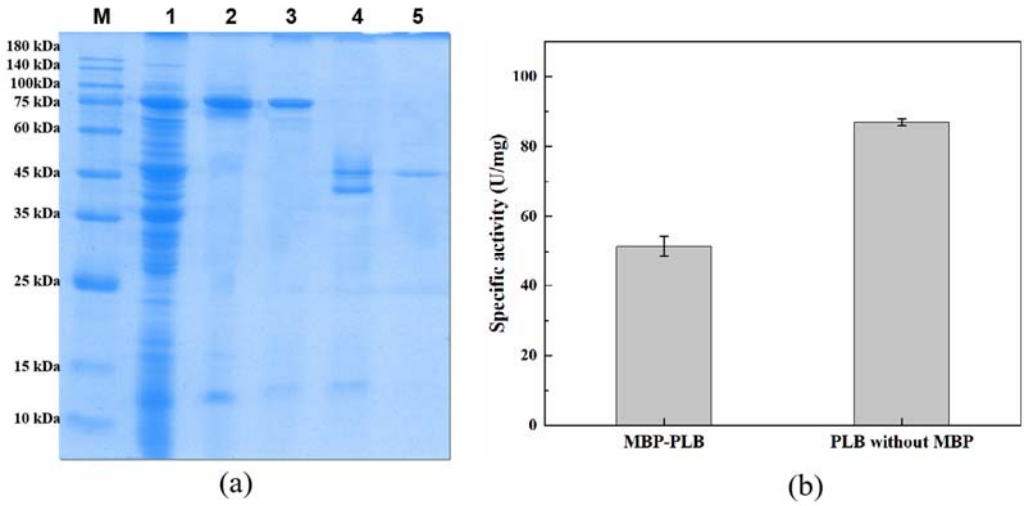

Figure 2. Effect of maltose-binding protein (MBP) as fusion partner on recombinant PLB. (**a**) SDS-PAGE analysis and (**b**) enzyme activity of PLB. Lane M: protein molecular weight marker; lane 1: supernatant of *E. coli* BL21(DE3)/pMal-c5x-PLB; lane 2: precipitation of *E. coli* BL21(DE3)/pMal-c5x-PLB; lane 3: eluted protein; lane 4: mixture with factor Xa; lane 5: PLB cleaved from MBP.

Subsequently, the effects of molecular chaperones on PLB were investigated. The different chaperones, including trigger factor (Tf), GroELS complex, DnaKJE complex, GroELS and DnaKJE, or GroELS and Tf, were co-expressed with PLB, which resulted in increased protein concentration and percentage of soluble PLB to some extent (Table S1). Co-expressing with DnaKJE obtained the highest soluble PLB. Meanwhile, SDS-PAGE analysis revealed that the lowest amount of inclusion bodies formed in the recombinant *E. coli* co-expressed with DnaKJE (Figure 3). Furthermore, specific activities of PLB were determined. The results showed that co-expression with different chaperones led to varying enhancement of PLB activity, and the crude enzyme of PLB co-expressed with the DnaKJE complex exhibited the highest level of PLB activity (186.50 ± 2.12 U/mg). These findings suggest that co-expression with molecular chaperones helped improve the production and enzyme activity of PLB. Molecular chaperones can prevent the protein from aggregating and rescue aggregated proteins. Among them, DnaKJE can bind to nascent proteins in unfolded states to reduce aggregation and promote the proteolysis of misfolded proteins to prevent the formation of inclusion bodies [25–27]. After further purification, PLB reached a maximum activity of 250.00 ± 3.23 U/mg, which was a 13.28-fold enhancement compared with the original PLB.

Overall, MBP-fused PLB promoted protein solubility and enzyme activity of PLB, but the specific protease (Factor Xa) had to be uesd to obtain PLB without MBP, incurring additional costs. In addition, the molecular chaperone DnaKJE had a more positive promoting effect on the enzyme activity of PLB. Therefore, the recombinant *E. coli* expressing the PLB simultaneously with the DnaKJE was selected for further production of PLB in our subsequent study.

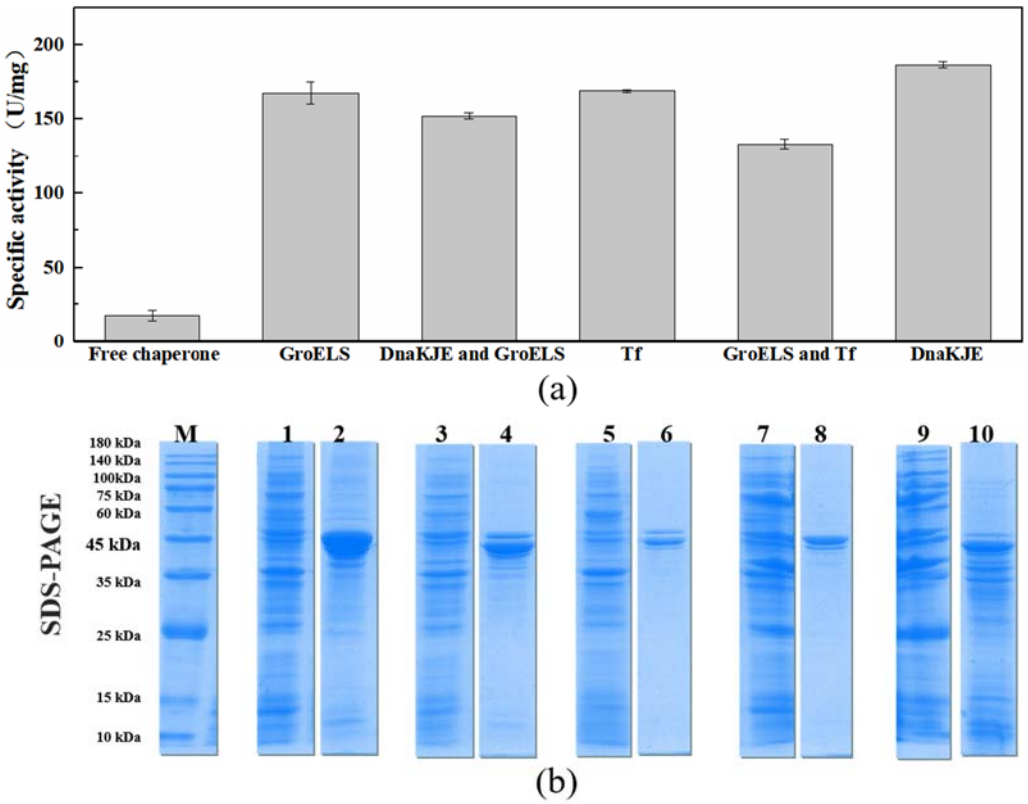

Figure 3. Effect of different molecular chaperones on recombinant PLB. (**a**) Enzyme activity and (**b**) SDS-PAGE analysis of PLB expressed in *E. coli* BL21(DE3) with the co-expression of chaperone plasmids. Lane M: protein molecular weight marker; lanes 1 and 2: supernatant and precipitation of *E. coli* BL21(DE3)/pET28a-PLB-pGro7 (containing GroELS); lanes 3 and 4: supernatant and precipitation of *E. coli* BL21(DE3)/pET28a-PLB-pG-KJE8 (containing GroELS and DnaKJE); lanes 5 and 6: supernatant and precipitation of *E. coli* BL21(DE3)/pET28a-PLB-pTf16 (containing Tf); lanes 7 and 8: supernatant and precipitation of *E. coli* BL21(DE3)/pET28a-PLB-pG-Tf2 (containing GroELS and Tf); lanes 9 and 10: supernatant and precipitation of *E. coli* BL21(DE3)/pET28a-PLB-pKJE7 (containing DnaKJE).

2.3. Optimizing the Expression Conditions for High-Level Soluble Production of PLB

In the cultivation stage, the parameters of the induction condition have essential effects on soluble protein yields and enzyme activity [28]. To further improve the activity of recombinant PLB, incubation temperature, incubation OD_{600}, IPTG concentration, and incubation time were optimized. By evaluating the PLB activity at incubation temperatures of 20 °C, 25 °C, 28 °C, 30 °C, and 37 °C, the optimum activity was determined at 25 °C (Figure 4a). It was shown that the lower incubation temperature led to a slower translation rate to favor the correct folding of the protein, thereby increasing the protein solubility and activity [29]. However, an excessively low temperature could result in a reduction in biomass, compromising protein yield. Compared to the PLB activity at an incubation OD_{600} of 0.2–1.0, the optimal time of IPTG addition was an OD_{600} of 0.8 (Figure 4b). The effect of IPTG concentration on PLB activity is shown in Figure 4c. The results show that the PLB activity was highest at the final IPTG concentration of 0.2 mM. With increased IPTG concentration, inclusion bodies formed more easily, decreasing enzyme activity. Finally, the induction time was optimized from 3–15 h (Figure 4d). The relative enzyme activity of PLB peaked at 9 h. The results indicate that optimizing the expression conditions of PLB can effectively improve the activity of PLB. These efforts led to the maximum enzyme activity of purified PLB reaching 524.64 ± 3.28 U/mg under the optimized induction conditions, which had a significant advantage over other reported PLB derived from

Bacillus velezensis (237 U/mg) [2], *Talaromyces marneffei* (48 U/mg) [30], and *Thermotoga lettingae* (158 U/mg) [31].

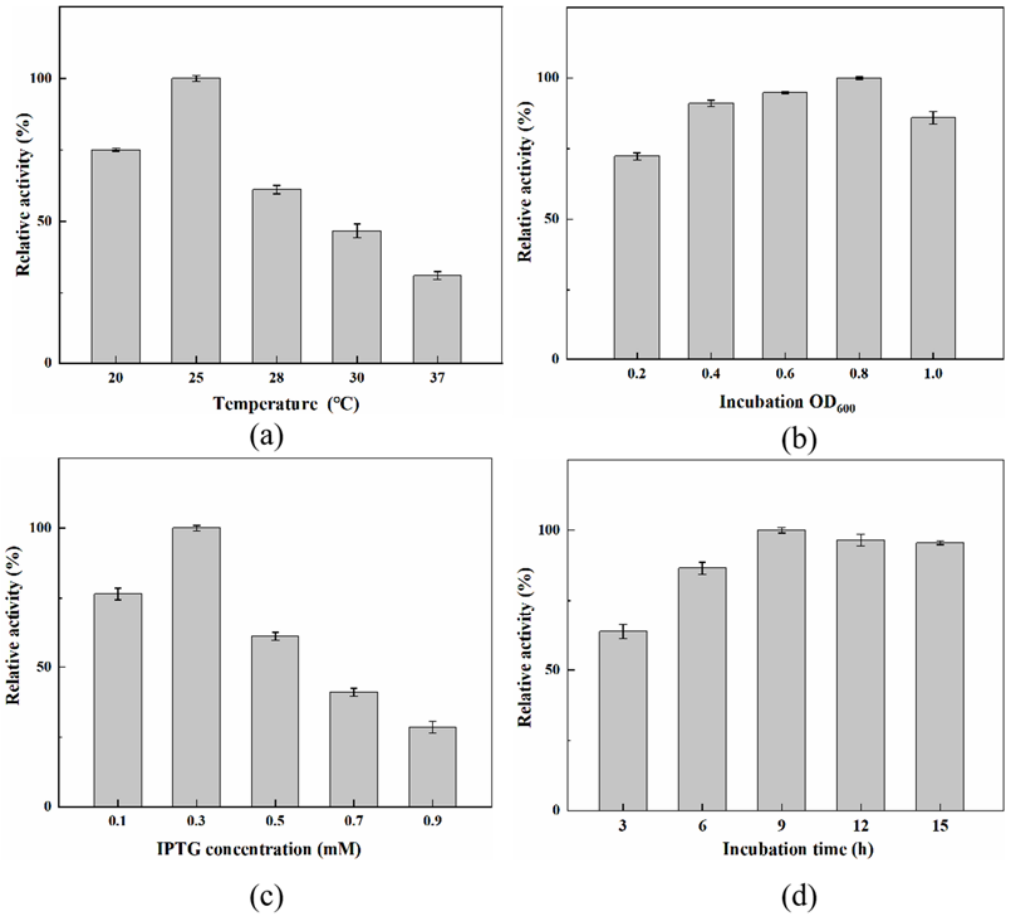

Figure 4. Effects of expression conditions on PLB activity. (**a**) Induction temperature; (**b**) induction OD_{600}; (**c**) IPTG concentration; and (**d**) induction time. "Relative activity" represents the change in PLB activity under various reaction conditions of single-factor alteration compared with that under the control reaction condition (temperature, 25 °C; incubation OD_{600}, 0.8; IPTG, 0.3 mM; and incubation time, 9 h).

2.4. Construction of a PLB-Catalyzed Hydrolysis System for L-α-GPC Synthesis

PLB harboring the activity of the sn-1 and sn-2 fatty acid ester hydrolase can be applied in catalytic production of L-α-GPC from PC as the substrate through the hydrolysis of both sn-1 and sn-2 acyl ester bonds [6]. However, PLB from *P. fluorescens* has not been applied in L-α-GPC synthesis, and the PLB-catalyzed hydrolysis system has not been systematically explored. As organic solvent was commonly added to the PLA_1-catalyzed system to improve the solubility of PC, the effects of six different organic solvents (isooctane, *n*-heptane, *n*-hexane, *n*-butanol, methanol, and dichloromethane) on PLB-catalyzed synthesis L-α-GPC were first investigated. As shown in Figure 5a, the highest titer and yield of L-α-GPC were obtained in aqueous (water) medium (5.2 g/L and 76.68%), whereas a small amount of L-α-GPC was detected in organic-aqueous mixed medium. An *n*-hexane-water biphasic system was reported to hydrolyze PC using PLA_1 as the biocatalyst, achieving a higher level of L-α-GPC productivity than aqueous medium [7,19]. However, our results indicate that PLB exhibited poor tolerance to organic solvents. Among them, L-α-GPC was not even detected in *n*-butanol-water biphasic medium and methanol-water homogenous medium because the addition of organic solvents also affected enzyme activity. Methanol (log *P* −0.76) and *n*-butanol (log *P* 0.8) have lower log *P* values than other organic solvents, such as *n*-heptane (log *P* 4.0) and *n*-hexane (log *P* 3.5). Organic solvents with low log *P*

values cause enzyme inactivation, whereas those with high log *P* values block binding and interaction between the enzyme and the substrate [30,32]. In addition, the structure of PLB from *P. fluorescens* shows that the hydrophilic C terminal of PLB is located on the surface, and the hydrophobic N terminal is located in the interior, whereas PLB is generally hydrophilic [33]. This might be the reason why PLB catalyzed well in water. The difference between PLB and PLA_1 illustrates the necessity of studying the PLB-catalyzed hydrolysis system.

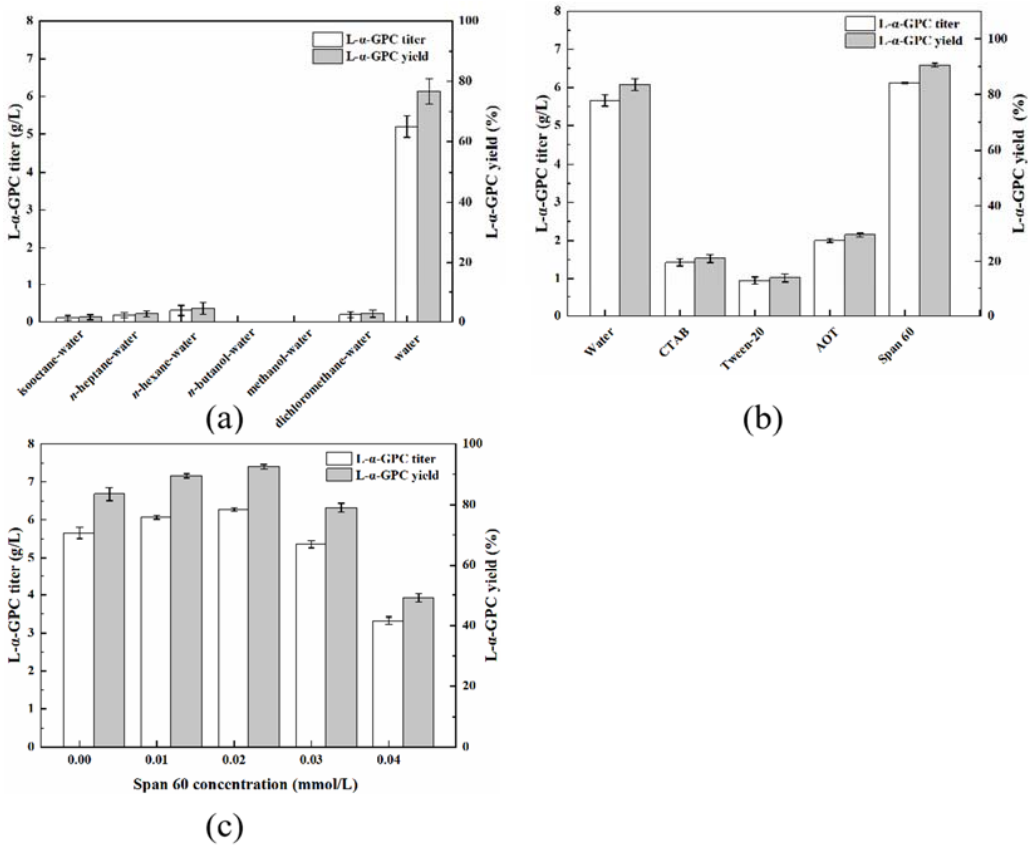

Figure 5. Construction of the PLB-catalyzed hydrolysis system for L-α-GPC synthesis. Effects of (**a**) organic solvents, (**b**) surfactants, and (**c**) Span 60 concentration on L-α-GPC production.

The use of a surfactant is a potential strategy to enhance the solubility and dispersibility of hydrophobic compounds and has been reported to enhance the efficiency of bioprocess [34]. In this work, cetrimonium bromide (CTAB), Tween 20, aerosol OT (AOT), and Span 60 were supplemented to investigate their effects on L-α-GPC production. Among them, Span 60 boosted the titer and yield of L-α-GPC (Figure 5b). The Span 60 concentration was optimized in a range from 0 to 0.04 mmol/L. The result is shown in Figure 5c. The highest titer of L-α-GPC was 6.27 g/L, with the highest yield achieved with a Span 60 concentration of 0.02 mmol/L. Span 60 is a nonionic surfactant, acting on the interface between the aqueous phase and the substrate to decrease interfacial tension and promote the solubility and dispersion of PC in the form of a nonionic surfactant micelle aqueous solution [7,35]. The lower hydrophile-lipophile balance (HLB) and solubility of Span 60 (HLB = 4.7) suggest that Span 60 was more hydrophobic and tended to arrange reverse micelle in aqueous media in comparison with other surfactants, such as CTAB (HLB = 15.8) and Tween 20 (HLB = 16.7) [36,37]. The amount of addition of Span 60 was greater than the critical micelle concentration (CMC) of Span 60 in order to ensure the formation of reverse micelles [36]. This form caused PLB in the water phase microenvironment into the hydrophobic environment of the substrate, improved the substrate concentration around PLB to increase the PLB and substrate contact opportunities, and promoted catalytic effi-

ciency. In addition, micelle structure transitioned with respect to surfactant concentration. The interaction and concentration of surfactant in a reaction system also affected enzyme structure and activity [38,39]. Therefore, a decline in L-α-GPC yield appeared as the Span 60 concentration increased from 0.02 mmol/L to 0.04 mmol/L after increasing L-α-GPC yield in the range of Span 60 concentration from 0 to 0.02 mmol/L.

2.5. Effects of Reaction Conditions on L-α-GPC Synthesis in the PLB-Catalyzed Hydrolysis System

As the key parameters in the enzyme catalysis system, reaction conditions contribute significantly to enzyme activity and efficiency. Therefore, reaction conditions, including temperature, pH, metal ions, and substrate concentrations, were optimized to enhance L-α-GPC synthesis. Comparing the L-α-GPC production at different reaction temperatures ranging from 20 °C to 50 °C, the relative L-α-GPC titer at 40 °C reached the highest level (Figure 6a). The approximate optimal temperature was also observed for several different sources of PLB, such as *Saccharomyces cerevisiae* (40 °C) [6], *Candida utilis* (40 °C) [40], and *Cryptococcus neoformans* (37 °C) [41]. Next, pH values varying from 5.0 to 8.0 were tested to determine the optimal pH. As shown in Figure 6b, the relative L-α-GPC titer was highest at pH 6.0, which is consistent with the optimal pH for the enzyme activity of PLB from *P. fluorescens* as reported previously [12]. Little enzyme activity of PLB was retained in acidic (pH below 5.0) or alkaline environments (pH above 7.0), resulting in lower L-α-GPC production. We next supplied an additional 0.1 mM of metal ions ($CaCl_2$, $CuCl_2$, $BaCl_2$, $CoCl_2$, $ZnCl_2$, $MgCl_2$, KCl, $NiCl_2$, and $FeSO_4$) to investigate the effects of metal ions on L-α-GPC production at 40 °C and pH 6.0. Figure 6c shows that Ca^{2+}, Ba^{2+}, Zn^{2+}, and Mg^{2+} exhibited positive effects on L-α-GPC production, and the addition of Mg^{2+} resulted in the highest relative L-α-GPC titer, whereas Cu^{2+}, Co^{2+}, Ni^{2+}, and Fe^{2+} exhibited strongly negative effects. Mohamed et al. proposed that adding Mg^{2+} and Ca^{2+} can markedly activate the enzyme [42]. Unlike some PLAs that are strictly dependent on Ca^{2+}, PLB can be activated by adding a variety of metal ions, suggesting that the arrangement of the catalytic site may not present an exclusive structure for specific metal binding [16]. Moreover, divalent metal ions can form complexes with phospholipids that affect the hydration to the phosphate group [43–45]. Different metal ions and even concentrations have inconsistent effects on PLB from different sources [2,43,44]. The negative effects of Cu^{2+}, Co^{2+}, Ni^{2+}, and Fe^{2+} were also reported in other studies [2,30]. Jia et al. speculated that Cu^{2+} promoted cysteine auto-oxidation to generate disulfide bonds or sulfenic acid [2].

Finally, high substrate concentrations commonly inhibit biocatalytic efficiency due to poor substrate diffusion and dissolution but are necessary to maximize volumetric productivity. Therefore, substrate concentrations were increased from 10 to 100 g/L to investigate the effect on L-α-GPC production at 40 °C and pH 6.0 with 0.1 mmol/L of Mg^{2+}. The result is shown in Figure 6d. A comparison of the L-α-GPC titer showed that the maximum was 16.91 ± 0.28 g/L when the substrate concentration was 60 g/L. High L-α-GPC yields (more than 80%) were achieved with a substrate concentration in the range of 10 to 60 g/L, reaching a maximum of 90.50 ± 2.21%, which is similar to the attractive yield reported by Jia et al. (L-α-GPC yield of 92.7% catalyzed by PLB from *B. velezensis*) and significantly superior to that of 17% catalyzed by PLB from *Saccharomyces cerevisiae* [2,6]. Compared to the low substrate concentration (10–20 g/L) employed in other studies [2,6], our Span-60-supplemented aqueous system achieved a high L-α-GPC yield at a high substrate concentration. The function of Span 60 might result in the maintenance of good catalytic efficiency at relatively high substrate concentrations with more positive effects (increased yield by 24.71% at a substrate concentration of 60 g/L). This excellent catalytic efficiency demonstrates high potential for industrial production of L-α-GPC. In a future study, protein engineering of PLB could be implemented, and the relevant catalytic processes need to be further optimized to meet industrial requirements.

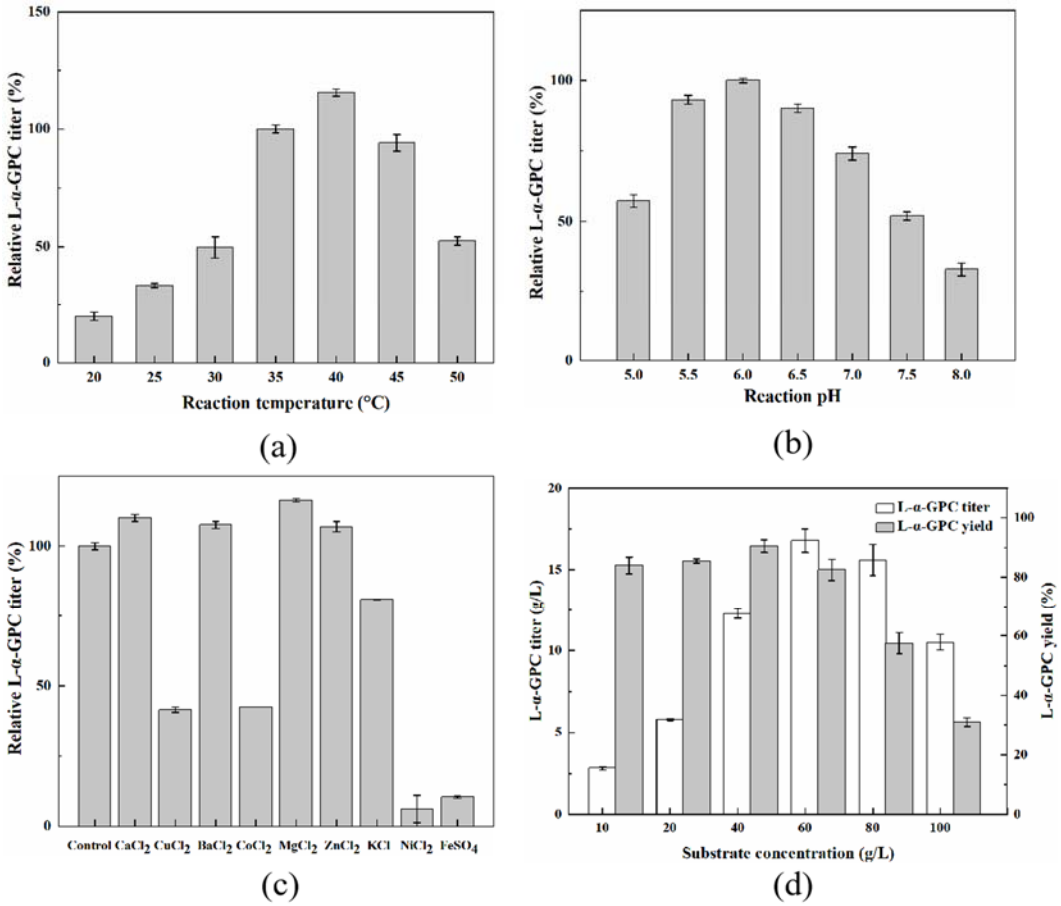

Figure 6. Optimization of L-α-GPC production. Effects of (**a**) reaction temperature, (**b**) reaction pH, (**c**) metal ions, and (**d**) substrate concentration on L-α-GPC production. "Relative L-α-GPC titer" represents the change in L-α-GPC titer under various reaction conditions of single-factor alteration compared with that under the control reaction condition (temperature, 40 °C; pH, 6.0; free metal ions).

3. Materials and Methods

3.1. Bacterial Strains and Culture Conditions

In this work, *E. coli* BL21(DE3) cells were used as hosts; the plasmids used and constructed are listed in Table 1. The codon-optimized coding sequence of PLB from *P. fluorescens* (accession: AEB15975) was synthesized by Tsingke Biological Technology (Beijing, China) and cloned into pET28a to obtain the recombinant plasmid pET28a-PLB. PMal-c5x, a maltose-binding protein (MBP)-tagged fusion protein expression vector containing MBP (accession: AAB87675.1), was used for the expression of MBP-fused PLB by constructing the recombinant plasmid pMal-c5x-PLB, in which the synthetic codon-optimized coding gene sequence of PLB was inserted between *Nco* I and *Bam* HI sites. Then, pET28a-PLB and pMal-c5x-PLB were transformed into *E. coli* BL21(DE3) to obtain the recombinant strains *E. coli* BL21(DE3)/pET28a-PLB and *E. coli* BL21(DE3)/pMal-c5x-PLB, respectively. The chaperone plasmids pTf16, pKJE7, pGro7, pG-Tf2, and pGKJE8 (Takara, Kyoto, Japan) were used for chaperone expression and co-transformed with pET28a-PLB into *E. coli* BL21(DE3) to obtain the recombinant *E. coli* strains for PLB expression.

Table 1. Strains and plasmids used in this work.

Strains or Plasmids	Description	Source
Strains		
E. coli BL21(DE3)	Used as host strain	Invitrogen
E. coli BL21(DE3)/pET28a-PLB	*E. coli* BL21(DE3) harboring plasmid pET 28a-PLB	This work
E. coli BL21(DE3)/pMal-c5x-PLB	*E. coli* BL21(DE3) harboring plasmid pMal-c5x-PLB	This work
E. coli BL21(DE3)/pET28a-PLB-pGro7	*E. coli* BL21(DE3) harboring plasmids pET 28a-PLB and pGro7	This work
E. coli BL21(DE3)/pET28a-PLB-pG-KJE8	*E. coli* BL21(DE3) harboring plasmids pET 28a-PLB and pG-KJE8	This work
E. coli BL21(DE3)/pET28a-PLB-pTf16	*E. coli* BL21(DE3) harboring plasmids pET 28a-PLB and pTf16	This work
E. coli BL21(DE3)/pET28a-PLB-pG-Tf2	*E. coli* BL21(DE3) harboring plasmids pET 28a-PLB and pG-Tf2	This work
E. coli BL21(DE3)/pET28a-PLB-pKJE7	*E. coli* BL21(DE3) harboring plasmids pET 28a-PLB and pKJE7	This work
Plasmids		
pET 28a	Expression vectors, Km^R, PT7, f1 ori	Invitrogen
pET 28a-PLB	The synthetic codon-optimized coding sequence of PLB from *Pseudomonas fluorescens* inserted between *Nco* I and *Xho* I sites of pET28	This work
pMal-c5x	Expression vector, Amp^R, lacIq, ORF MBP, Fx, ori	NEB
pMal-c5x-PLB	The synthetic codon-optimized coding sequence of PLB inserted between *Nco* I and *Bam* HI sites of pMal-c5x	This work
pTf16	tig, Cm^R, araB, pACYC ori	TaKaRa
pKJE7	dnaK-dnaJ-grpE, Cm^R, araB, pACYC ori	TaKaRa
pGro7	groES-groEL, Cm^R, araB, pACYC ori	TaKaRa
pG-Tf2	groES-groEL-tig, Cm^R, Pzt-1, pACYC ori	TaKaRa
pG-KJE8	dnaK-dnaJ-grpE, groES-groEL, Cm^R, araB, Pzt-1, pACYC ori	TaKaRa

Strains were activated via overnight culture at 37 °C and were then inoculated into 100 mL of Luria-Bertani (LB) medium supplemented with the corresponding antibiotics (50 μg/mL kanamycin for *E. coli* BL21(DE3)/pET28a-PLB, 100 μg/mL ampicillin for *E. coli* BL21(DE3)/pMal-c5x-PLB, and 50 μg/mL kanamycin and 34 μg/mL chloramphenicol for the recombinant *E. coli* strains harboring pET28a-PLB and different chaperone expression plasmid). After growing to the optical density (OD_{600}) of 0.6 at 37 °C with shaking at 200 rpm, 0.5 mmol/L isopropyl-beta-D-thiogalactopyranoside (IPTG) was added to induce PLB expression. L-arabinose and/or tetracycline were added when molecular chaperones were needed to be induced for expression. After 8–10 h of incubation at 28 °C and 200 rpm, the cells were harvested by centrifugation for 10 min at 4 °C and washed twice with phosphate-buffered saline (PBS) (pH 7.0) for subsequent experiments. To improve the soluble protein yields and enzyme activity of PLB, incubation OD_{600} values of 0.2–1.0, IPTG concentrations of 0.1–0.9 mmol/L, incubation temperatures of 20–37 °C, and induction times of 3–15 h were investigated.

3.2. Sodium Dodecyl Sulfate-Polyacrylamide Gel Electrophoresis (SDS-PAGE) Analysis and Purification of PLB

The cells were suspended with PBS buffer (pH 7.0, OD_{600} = 15), sonicated for 15 min, and centrifuged into supernatant and precipitation (15 min, 4000× *g*, 4 °C). A 20 μL protein solution was added with 6 × protein loading buffer and denatured at 99 °C for 10 min. The protein concentration was determined by Bradford's method. SDS-PAGE with 12.5% (*w*/*v*) separating gel was performed with a Bio-Rad Mini-Protean Tetra cell (Bio-Rad, Hercules, CA, USA) to analyze the soluble proteins in the supernatant, as well as precipitation. After staining with Coomassie Brilliant Blue, the stained gels were scanned, and the protein bands were quantified by scanning the gels using a Bio-Rad imaging system (Model Universal Hood II, Bio-Rad Laboratories, Hercules, CA, USA). Because the pET-28a carried the His tag sequence, the expressed soluble PLB with the 6-His tag was purified using an Ni-nitrilotriacetic acid affinity chromatography (Ni–NTA) column equilibrated with 20 mmol/L Tris-HCl buffer containing 50 mmol/L imidazole. After elution using 50 mmol/L Tris-HCl buffer containing 500 mmol/L imidazole, the target PLB

was concentrated and washed to remove imidazole. PLB fused to MBP was expressed in *E. coli* BL21(DE3)/pMal-c5x-PLB and then purified using HiCap dextrin filled with 6FF dextrin beads (Smart-lifesciences, China) via MBP affinity chromatography. The HiCap dextrin was equilibrated with lysis buffer containing 20 mmol/L Tris-HCl, 200 mmol/L NaCl, and 1 mmol/L EDTA (pH 7.4). MBP fusion PLB was loaded and eluted using elution buffer containing 20 mmol/L Tris-HCl, 1 mmol/L EDTA, and 10 mmol/L maltose (pH 7.4). Protein was quantified by Bradford assay and subjected to SDS-PAGE analysis.

3.3. Enzymatic Assays

The activity of PLB was measured as previously reported by Jiang et al. [46]. The reaction system consisted of 10 g/L of egg yolk lecithin powder (approximately 70% PC and 15% phosphatidylethanolamine) (Merya's Lecithin Co., Beijing, China) and 0.6 mg/mL PLB in 200 mmol/L PBS buffer. The reaction was incubated at 30 °C with shaking at 200 rpm for 30 min and then terminated by adding absolute ethyl alcohol. A concentration of 50 mmol/L of NaOH was used to titrate the liberated fatty acids. One unit of PLB (U) was defined as the amount of enzyme that released 1 μmol of free fatty acids per minute under the described conditions. All experiments were performed in triplicate.

3.4. Production of L-α-GPC from PC Using PLB as the Catalyst

The reaction system of L-α-GPC enzymatic production from PC using PLB was composed of 1 g/L of PLB, 20 g/L of egg yolk lecithin powder and 0.01 mmol/L surfactant (cetrimonium bromide (CTAB), Tween 20, aerosol OT (AOT), and Span 60) in pure water medium or a mixture of different organic solvents (isooctane, *n*-heptane, *n*-hexane, *n*-butanol, methanol, and dichloromethane) and water (1:1, *v*/*v*) in an organic-aqueous mixed medium. The control reaction system contained only PLB and PC in pure water. To optimize the synthesis of L-α-GPC, different concentrations of Span 60 were added to the reaction system and incubated at 20 °C, 25 °C, 30 °C, 35 °C, 40 °C, 45 °C, or 50 °C for 8 h. The optimal reaction pH was confirmed in the range of pH 5.0 to 8.0. Metal ions, including 0.1 mmol/L of $CaCl_2$, $CuCl_2$, $BaCl_2$, $CoCl_2$, $ZnCl_2$, $MgCl_2$, KCl, $NiCl_2$, and $FeSO_4$, were used to investigate the effect of metal ions on L-α-GPC production at 40 °C and pH 6.0. On this basis, the substrate concentration in the range of 10 to 100 g/L was further optimized for the synthesis of L-α-GPC at 40 °C and pH 6.0 with 0.1 mmol/L of Mg^{2+}. Following the reaction, samples were treated according to methods described in the literature for HPLC analysis [19]. All experiments were performed in triplicate.

3.5. HPLC Analysis

The concentrations of PC and L-α-GPC were measured according to a previously reported method [7,19]. Specifically, a 1260 series high-performance liquid chromatography (HPLC) system (Agilent Technologies, Santa Clara, CA, USA) was equipped with a ZORBAX RX-SIL column (250 mm × 4.6 mm, 5 um i.d., Agilent Technologies, Santa Clara, CA, USA) to separate PC and L-α-GPC, as well as an evaporative light-scattering detector (ELSD). ELSD-HPLC analysis was carried out as follows. The column and drift tube temperatures were maintained at 25 °C and 65 °C, respectively. The mobile phase composed of methanol and water (9:1, *v*/*v*) was employed at a flow rate of 1 mL/min. The flow rate of nitrogen was 1.5 SLM. The yield of L-α-GPC was calculated by dividing the final L-α-GPC amount (the final L-α-GPC concentration multiplied by reaction volume) by the theoretical L-α-GPC amount [2,7].

4. Conclusions

In this work, high-level active PLB was produced by enhancing soluble expression of PLB in *E. coli* and used for efficient synthesis of L-α-GPC. PLB from *P. fluorescens* was heterologously expressed in *E. coli* BL21(DE3), and five different molecular chaperones or MPB were used to minimize inclusion body formation, consequently obtaining highly active PLB. By comparing the enzyme activity of PLB, co-expression of PLB and DnaKJE was identified

as the best expression strategy. After optimization of expression conditions, purified PLB activity reached 524.64 ± 3.28 U/mg. Subsequently, an effective PLB-catalyzed system for L-α-GPC synthesis was established by comparing the L-α-GPC yield of reactions in six organic-aqueous mixed media and four surfactant-supplemented aqueous media, followed by investigation of appropriate reaction conditions. Finally, the highest yield of L-α-GPC was found to be up to 90.50 ± 2.21%. Based on our findings, the co-expression of molecular chaperones can be applied to increase the production of PLB used for efficient catalytic production of L-α-GPC. Such an attractive yield in an aqueous medium demonstrates the potential for industrial applications.

Supplementary Materials: The following supporting information can be downloaded at: https://www.mdpi.com/article/10.3390/catal12060650/s1, Figure S1: SDS-PAGE analysis of the supernatant of recombinant strains containing chaperone plasmids; Figure S2: SDS-PAGE analysis of the precipitation of recombinant strains containing chaperone plasmids; Figure S3: SDS-PAGE analysis of purified PLB; Table S1: Protein concentration and the percent of soluble PLB protein.

Author Contributions: Data curation, Y.L.; methodology, W.Y.; formal analysis, J.F.; investigation, H.L. and S.X.; writing—original draft preparation, J.F.; writing—review and editing, J.F. and X.W.; project administration, X.W.; funding acquisition, J.F., S.X., X.W. and K.C. All authors have read and agreed to the published version of the manuscript.

Funding: This research was funded by the National Key Research and Development Program of China (2018YFA0901500), the National Science Foundation of Young Scientists of China (Grant Nos. 22108123, 21908099), and the China Postdoctoral Science Foundation (No. 2020M681569).

Data Availability Statement: Not applicable.

Conflicts of Interest: The authors declare no conflict of interest.

Sample Availability: Not available.

References

1. Du, Y.W.; He, W.; Zhou, W.Y.; Li, X.S. Disulfide phosphatidylcholines: Alternative phospholipids for the preparation of functional liposomes. *Chem. Commun.* **2019**, *55*, 8434–8437. [CrossRef] [PubMed]
2. Jia, L.G.; Wang, C.; Wu, Y.F.; Ma, X.Y.; Zhang, X.; Chu, X.X.; Lu, F.P.; Liu, Y.H. Production of L-alpha-glycerylphosphorylcholine from oil refining waste using a novel cold-active phospholipase B from *Bacillus velezensis*. *ACS Sustain. Chem. Eng.* **2021**, *9*, 13337–13346. [CrossRef]
3. Lee, S.H.; Choi, B.Y.; Kim, J.H.; Kho, A.R.; Sohn, M.; Song, H.K.; Choi, H.C.; Suh, S.W. Late treatment with choline alfoscerate (L-alpha glycerylphosphorylcholine, alpha-GPC) increases hippocampal neurogenesis and provides protection against seizure-induced neuronal death and cognitive impairment. *Brain. Res.* **2017**, *1654*, 66–76. [CrossRef] [PubMed]
4. Tayebati, S.K. Phospholipid and lipid derivatives as potential neuroprotective compounds. *Molecules* **2018**, *23*, 2257. [CrossRef]
5. Park, J.M.; De Castro, K.A.; Ahn, H.; Rhee, H. Facile syntheses of L-alpha-glycerophosphorylcholine. *B. Korean. Chem. Soc.* **2010**, *31*, 2689–2691. [CrossRef]
6. Liu, Y.H.; Li, M.J.; Huang, L.; Gui, S.; Jia, L.B.; Zheng, D.; Fu, Y.; Zhang, Y.T.; Rui, J.Q.; Lu, F.P. Cloning, expression and characterisation of phospholipase B from *Saccharomyces cerevisiae* and its application in the synthesis of L-alpha-glycerylphosphorylcholine and peanut oil degumming. *Biotechnol. Biotec. Equip.* **2018**, *32*, 968–973. [CrossRef]
7. Lu, Y.Y.; Zhang, A.L.; Wang, X.; Hao, N.; Chen, K.Q.; Ouyang, P.K. Surfactant enhanced l-alpha-glycerylphosphorylcholine production from phosphatidylcholine using phospholipase A(1) in the aqueous phase. *Biocatal. Biotransfor.* **2019**, *37*, 361–366. [CrossRef]
8. Másson, M.; Loftsson, T.; Haraldsson, G. Marine lipids for prodrugs, soft compounds and other pharmaceutical applications. *Pharmazie* **2000**, *3*, 172–177.
9. Zhang, K.Y.; Liu, Y.F.; Wang, X.G. Enzymatic preparation of L-alpha-glycerylphosphorylcholine in an aqueous medium. *Eur. J. Lipid. Sci. Tech.* **2012**, *114*, 1254–1260. [CrossRef]
10. Lim, C.W.; Kim, B.H.; Kim, I.H.; Lee, M.W. Modeling and optimization of phospholipase A(1)-catalyzed hydrolysis of phosphatidylcholine using response surface methodology for lysophosphatidylcholine production. *Biotechnol. Prog.* **2015**, *31*, 35–41. [CrossRef]
11. Li, H.; Cao, X.; Lu, Y.Y.; Ni, Y.; Wang, X.; Lu, Q.H.; Li, G.L.; Chen, K.Q.; Ouyang, P.K.; Tan, W.M. Alkaline modification of a metal-enzyme-surfactant nanocomposite to enhance the production of L-alpha-glycerylphosphorylcholine. *Catalysts* **2019**, *9*, 237. [CrossRef]

12. Jiang, F.Y.; Huang, S.; Imadad, K.; Li, C. Cloning and expression of a gene with phospholipase B activity from Pseudomonas fluorescens in *Escherichia coli*. *Bioresour. Technol.* **2012**, *104*, 518–522. [CrossRef] [PubMed]
13. Jiang, F.Y.; Wang, J.M.; Ju, L.C.; Kaleem, I.; Dai, D.Z.; Li, C. Optimization of degumming process for soybean oil by phospholipase B. *J. Chem. Technol. Biot.* **2011**, *86*, 1081–1087. [CrossRef]
14. Huang, S.; Liang, M.L.; Xu, Y.H.; Rasool, A.; Li, C. Characteristics and vegetable oils degumming of recombinant phospholipase B. *Chem. Eng. J.* **2014**, *237*, 23–28. [CrossRef]
15. Ullah, A.; Masood, R. The sequence and three-dimensional structure characterization of snake venom phospholipases B. *Front. Mol. Biosci.* **2020**, *7*, 175. [CrossRef]
16. Kohler, G.A.; Brenot, A.; Haas-Stapleton, E.; Agabian, N.; Deva, R.; Nigam, S. Phospholipase A(2) and phospholipase B activities in fungi. *BBA-Mol. Cell Biol. Lipids* **2006**, *1761*, 1391–1399. [CrossRef] [PubMed]
17. Xu, S.Y.; Zhao, L.S.; Larsson, A.; Venge, P. The identification of a phospholipase B precursor in human neutrophils. *FEBS J.* **2009**, *276*, 175–186. [CrossRef]
18. Cai, Z.Z.; Wang, H.F.; Li, W.Z.; Lee, W.J.; Li, W.; Wang, Y.; Wang, Y. Preparation of L-alpha-glyceryl phosphorylcholine by hydrolysis of soy lecithin using phospholipase A1 in a novel solvent-free water in oil system. *LWT-Food. Sci. Technol.* **2020**, *129*, 109562. [CrossRef]
19. Bang, H.J.; Kim, I.H.; Kim, B.H. Phospholipase A(1)-catalyzed hydrolysis of soy phosphatidylcholine to prepare L-alpha-glycerylphosphorylcholine in organic-aqueous media. *Food. Chem.* **2016**, *190*, 201–206. [CrossRef]
20. San-Miguel, T.; Perez-Bermudez, P.; Gavidia, I. Production of soluble eukaryotic recombinant proteins in *E-coli* is favoured in early log-phase cultures induced at low temperature. *Springerplus* **2013**, *2*, 89. [CrossRef]
21. García-Fruitós, E. *Insoluble Proteins*; Humana Press: New York, NY, USA, 2015; pp. 1–24.
22. Fox, J.D.; Kapust, R.B.; Waugh, D.S. Single amino acid substitutions on the surface of *Escherichia coli* maltose-binding protein can have a profound impact on the solubility of fusion proteins. *Protein Sci.* **2001**, *10*, 622–630. [CrossRef]
23. Raran-Kurussi, S.; Keefe, K.; Waugh, D.S. Positional effects of fusion partners on the yield and solubility of MBP fusion proteins. *Protein Expres. Purif.* **2015**, *110*, 159–164. [CrossRef] [PubMed]
24. Raran-Kurussi, S.; Waugh, D.S. The ability to enhance the solubility of its fusion partners is an intrinsic property of maltose-binding protein but their folding is either spontaneous or chaperone-mediated. *PLoS ONE* **2012**, *7*, e49589. [CrossRef]
25. Yoshimune, K.; Ninomiya, Y.; Wakayama, M.; Moriguchi, M. Molecular chaperones facilitate the soluble expression of N-acyl-D-amino acid amidohydrolases in *Escherichia coli*. *J. Ind. Microbiol. Biotechnol.* **2004**, *31*, 421–426. [CrossRef] [PubMed]
26. Cui, S.S.; Lin, X.Z.; Shen, J.H. Effects of co-expression of molecular chaperones on heterologous soluble expression of the cold-active lipase Lip-948. *Protein Expres. Purif.* **2011**, *77*, 166–172.
27. Farajnia, S.; Ghorbanzadeh, V.; Dariushnejad, H. Effect of molecular chaperone on the soluble expression of recombinant fab fragment in *E. coli*. *Int. J. Pept. Res. Ther.* **2020**, *26*, 251–258. [CrossRef]
28. Falak, S.; Sajed, M.; Rashid, N. Strategies to enhance soluble production of heterologous proteins in *Escherichia coli*. *Biologia* **2022**, *77*, 893–905. [CrossRef]
29. Vera, A.; Gonzalez-Montalban, N.; Aris, A.; Villaverde, A. The conformational quality of insoluble recombinant proteins is enhanced at low growth temperatures. *Biotechnol. Bioeng.* **2007**, *96*, 1101–1106. [CrossRef]
30. Durrani, R.; Khan, F.I.; Ali, S.; Wang, Y.H.; Yang, B. A thermolabile phospholipase B from talaromyces marneffei GD-0079: Biochemical characterization and structure dynamics study. *Biomolecules* **2020**, *10*, 231. [CrossRef]
31. Wei, T.; Xu, C.P.; Yu, X.; Jia, W.W.; Yang, K.P.; Jia, C.X.; Mao, D.B. Characterization of a novel thermophilic phospholipase B from *Thermotoga lettingae* TMO: Applicability in enzymatic degumming of vegetable oils. *J. Ind. Microbiol. Biotechnol.* **2015**, *42*, 515–522. [CrossRef]
32. Uttatree, S.; Winayanuwattikun, P.; Charoenpanich, J. Isolation and Characterization of a Novel Thermophilic-Organic Solvent Stable Lipase from Acinetobacter baylyi. *Appl. Biochem. Biotechnol.* **2010**, *162*, 1362–1376. [CrossRef] [PubMed]
33. Zhao, Y.; Jiang, F.; Li, C.; Dai, D. Interfacial catalytic mechanism of *Pseudomonas fluorescens* phospholipase B. *CIESC J.* **2020**, *71*, 4255–4259.
34. Wang, Z.L. Bioavailability of organic compounds solubilized in nonionic surfactant micelles. *Appl. Microbiol. Biotechnol.* **2011**, *89*, 523–534. [CrossRef] [PubMed]
35. Hegde, R.R.; Kumar, S.; Aswal, V.K.; Verma, A.; Bhattacharya, S.S.; Ghosh, A. Small-angle neutron scattering study of nonionic surfactant micelles and phase transitions in w/o microemulsion. *J. Dispers. Sci. Technol.* **2014**, *35*, 783–788. [CrossRef]
36. Azam, S.; Kiana, P.; Abolfazl, S. How the CMC adjust the liquid mixture density and viscosity of non-ionic surfactants at various temperatures? *J. Mol. Liq.* **2022**, *347*, 117971.
37. Gacek, M.M.; Berg, J.C. Effect of surfactant hydrophile-lipophile balance (HLB) value on mineral oxide charging in apolar media. *J. Colloid. Interf. Sci.* **2015**, *449*, 192–197. [CrossRef]
38. Chin, M.; Somasundaran, P. Enzyme activity and structural dynamics linked to micelle fromation: A fluorescence anisotropy and ESR study. *Photochem. Photobiol.* **2014**, *90*, 455–462. [CrossRef]
39. Magalhaes, S.S.; Alves, L.; Sebastiao, M.; Medronho, B.; Almeida, Z.L.; Faria, T.Q.; Brito, R.M.M.; Moreno, M.J.; Antunes, F.E. Effect of ethyleneoxide groups of anionic surfactants on lipase activity. *Biotechnol. Progr.* **2016**, *32*, 1276–1282. [CrossRef]
40. Fujino, S.; Akiyama, D.; Akaboshi, S.; Fujita, T.; Watanabe, Y.; Tamai, Y. Purification and characterization of phospholipase B from *Candida utilis*. *Biosci. Biotech. Bioch.* **2006**, *70*, 377–386. [CrossRef]

41. Chen, S.C.A.; Wright, L.C.; Golding, J.C.; Sorrell, T.C. Purification and characterization of secretory phospholipase B, lysophospholipase and lysophospholipase/transacylase from a virulent strain of the pathogenic fungus *Cryptococcus neoformans*. *Biochem. J.* **2000**, *347*, 431–439. [CrossRef]
42. Mohamed, A.H.K.A.; Ayobe, M.H. Studies of phospholipase A and B activities of egyptian snake venoms and a scorpion toxin. *Toxicon* **1969**, *6*, 293–298. [CrossRef]
43. Matsumoto, Y.; Mineta, S.; Murayama, K.; Sugimori, D. A novel phospholipase B from Streptomyces sp. NA684—Purification, characterization, gene cloning, extracellular production and prediction of the catalytic residues. *FEBS J.* **2013**, *280*, 3780–3796. [CrossRef] [PubMed]
44. Altenbach, C.; Seelig, J. Calcium binding to phosphatidylcholine bilayers as studied by deuterium magnetic resonance. Evidence for the formation of a calcium complex with two phospholipid molecules. *Biochemistry* **1984**, *23*, 3913–3920. [CrossRef]
45. Binder, H.; Arnold, K.; Ulrich, A.S.; Zschornig, O. Interaction of Zn^{2+} with phospholipid membranes. *Biophys. Chem.* **2001**, *90*, 57–74. [CrossRef]
46. Jiang, F.Y.; Wang, J.M.; Kaleem, I.; Dai, D.Z.; Zhou, X.H.; Li, C. Degumming of vegetable oils by a novel phospholipase B from Pseudomonas fluorescens BIT-18. *Bioresour. Technol.* **2011**, *102*, 8052–8056. [CrossRef] [PubMed]